Chinese Journal of Physiology 61(2): 65-74, 2018
DOI: 10.4077/CJP.2018.BAG513

Inverse Correlation between Methylation and Expression of the Delta-like Ligand 1 Gene in Gastric Cancer

Chien-Heng Shen[1, *], Shui-Yi Tung[1, *], Min-Jen Tseng[2], and Yu-Wei Leu[2]

[1]Department of Hepato-Gastroenterology, Chang Gung Memorial Hospital, Chiayi 61363 and
[2]Human Epigenomics Center, Department of Life Science, Institute of Molecular Biology and Institute of Biomedical Science, National Chung Cheng University, Chiayi 62102, Taiwan, Republic of China

Abstract

Notch signaling is a candidate pathway that transmits environmental information into the cell and interferes with the epigenome of gastric cancer. This study aimed to explore if the Notch pathway was abnormally regulated during gastric tumorigenesis. To achieve the goal, Delta-like ligand 1 (*DLL1*) gene expression, Notch upstream signal, promoter methylation and its correlation with *DLL1* expression were examined by methylation-specific polymerase chain reaction (PCR) and real-time PCR (RT-PCR) in cultured gastric cancer cell lines or gastric cancer patient samples. Immunostainings and tissue arrays (n = 40) were used to confirm the *DLL1* expression was down-regulated in cancer cells. Transient or stable Notch1 active domain (NICD)-overexpression suppressed proliferation of the gastric cells but the *in vivo* tumor growth was enhanced. The results of abnormal *DLL1* methylation and expression observed in early gastric lesions and in gastric cancers may be relevant to the pathogenesis of gastric cancer.

Key Words: DNA methylation, gastric cancer, signal transduction, tissue array and epigenetics

Introduction

Gastric cancer is a global health problem, although its incidence is decreasing (23). Environmental factors, like *H. pylori* infection and a high-salt diet, are associated with gastric cancer onset, and signaling pathways are required to relay these outside signals into the cell (11, 24). Disruption of signaling pathways induced by detrimental environmental factors may be memorized by cells as a somatic inheritable epigenetic change that may provide a selective advantage for tumorigenesis (10, 12). The biological functions regulated by these pathways would then be altered in the cancer cells.

Together with Wnt and bone morphogenetic proteins (BMPs), Notch signals are critical for the determination of stemness in both embryonic and somatic stem cells (6). Notch signaling was initially found to regulate neuronal differentiation, and this role is conserved from *Drosophila* to humans (1, 5). Notch proteins are transmembrane receptors that are activated following interaction with Delta-like ligands (DLL) on neighboring cells, which triggers downstream Notch signaling (22). Therefore, abnormal DLL regulation is associated with consequent alterations in Notch activation (18). While aberrant Notch signaling has been found in breast, colorectal, glioblastoma, oral and lung cancers, but this pathway

Corresponding author: Dr. Yu-Wei Leu, Department of Life Science, Institute of Molecular Biology and Institute of Biomedical Science, National Chung Cheng University, Chiayi 62102, Taiwan, ROC. Tel: +886-5-2729330, Fax: +886-5-2722871, E-mail: bioywl@ccu.edu.tw.
*Contributed equally to this work.
Received: March 1, 2017; Revised (Final Version): December 19, 2017; Accepted: January 2, 2018.
 ISSN : 0304-4920. http://www.cps.org.tw

seems to play multiple roles in solid tumors ranging from being oncogenic or tumor suppressive, to contributing to tumor progression and maintenance (2, 11, 21). Some of these functions are contradictory under different contexts, which complicate the usage of the Notch signaling pathway as diagnostic or therapeutic targets (19). Little evidence regarding Notch signaling in gastric cancer has been reported; thus, the role of Notch in gastric tumorigenesis needs to be clarified (9, 15).

DNA methylation is a stable epigenetic mark that is inheritable in somatic cells; abnormal DNA methylation has been associated with tumorigenesis in various cancers (3, 25). Differential DNA methylation is one of the main determinants for genomic imprinting, genome stability and differentiation (4). Loss of global methylation and/or increased methylation within tumor suppressor genes have been hypothesized to result in transformation of somatic cells and have been demonstrated in a variety of cancers (7). As previously reported in the estrogen receptor (14), knockdown of upstream receptors could lead to downstream signaling-specific methylation (14). This inheritable methylation can pass on the signal-specific silencing to affect the function of the associated specific pathways in subsequent cellular generations (8). If the abnormal regulation and methylation of components of the Notch signaling pathway could be confirmed in gastric cancer, these methylation changes could be tracked to monitor gastric oncogenesis and progression.

In order to determine if changes in Notch signaling occur in gastric cancer, we sought to determine the methylation and expression status of the *DLL1* gene in gastric cancer. We performed methylation-specific polymerase chain reaction (PCR) (MSP) within the *DLL1* promoter region to determine if the treatment of the methylation inhibitor, 5-Aza-2'-deoxycytidine (5-Aza), could induce *DLL1* demethylation, and if *DLL1* expression was increased after 5-Aza treatment. In pre-cancerous gastric tissue samples, abnormal *DLL1* methylation was identified and abnormal *DLL1* expression was detected by immunostaining. To confirm the abnormal *DLL1* expression in gastric cancer, tissue arrays were employed. Finally, *Notch1* was overexpressed in gastric cancer cells to test if Notch signaling could interfere with tumor cell proliferation. These findings will help to decipher the role of Notch signaling in gastric tumorigenesis.

Materials and Methods

Human Samples

The human samples were collected under the regulation of CGMH IRB102-1999B, 103-2136 and 103-5491C and from the Tissue Bank, Department of Medical Research, Chang Gung Memorial Hospital, Chiayi. The gastric lesions used in this study are listed in Table 1.

Cell Culture

Human gastric cancer cell lines, including AGS, KATOIII, MKN28, MKN45, SNU1 and SNU16, were cultured with RPMI-1640 medium (Invitrogen, CA, USA) supplemented with 10% fetal bovine serum (Invitrogen), 100 mg/ml penicillin/streptomycin (Invitrogen), and 2 mM L-glutamine (Invitrogen).

5-Aza Treatment

Cells were treated with 5 μM 5-Aza (Sigma-Aldrich, MO, USA) or an equal volume of dimethyl sulfoxide, DMSO (Sigma-Aldrich) as a control for 5 consecutive days.

Bisulfite Conversion

Isolated genomic DNA (0.5 μg) was bisulfite-converted and purified as described by Yan *et al.* (26).

Relative Quantitative Real-Time MSP (qRT-MSP)

The relative qMSP was performed as described by Yan *et al.* (26). Briefly, bisulfite-converted genomic DNA was subjected to qRT-PCR with *DLL1* methylation-specific primers (Table 2). A SYBR Green I PCR Kit (Toyobo, Osaka, Japan) was used to conduct relative qMSP in an iQ5 qRT-PCR instrument (Bio-Rad, CA, USA). Analysis of the melting temperature was performed to ensure that a specific amplicon was generated during PCR. *Col2A1* (NM_033150) was used to generate a standard curve. The methylation percentage was calculated as: [mean of target gene]/[mean of *Col2A1*]. The fold change was then calculated as: [control or 5-Aza-treated DNA methylation percentage]/[control methylation percentage]. In order to observe the methylation fold changes in patient samples, the methylation fold changes were calculated as: [tumor parts or normal part methylation percentage]/[adjacent normal part DNA methylation percentage from the same patient].

Relative qRT-PCR

Total RNA was isolated (14) and 2 μg was reverse transcribed using SuperScript II reverse transcriptase (Invitrogen). qRT-PCR was performed using a SYBR Green I PCR Kit (Toyobo) in an iQ5 qRT-PCR instrument (Bio-Rad) with *DLL1* and glyceraldehyde-

Table 1. Collected gastric lesions

Biopsy	Diagnosis	*H. pylori*[#]	RC*
001	Adenocarcinoma, intestinal, poorly-differentiated, Pt2n0	+	-
002	Malignant, Diffuse large-B-cell lymphoma	-	+
003	Chronic inflammation with intestinal metaplasia	U	+
004	Adenocarcinoma, poorly-differentiated	-	+
005	Adenocarcinoma, moderately differentiated	-	+
006	Chronic inflammation	U	+
007	Erosion, Ectopic fundic glands	-	+
008	Chronic inflammation with intestinal metaplasia	-	+
009	Adenocarcinoma, poorly-differentiated, High-grade malignant tumor	+	+
010	Erosion	-	+
011	Highly atypical cells	-	+
012	Chronic active gastritis	-	+
013	Gastric cancer	U	-
014	Adenocarcinoma with cribriform component, pT3N3b	U	-
015	Adenocarcinoma, poorly differentiated	-	+
016	Ectopic parietal glands, c/w heterotopia	-	+
017	Signet ring cell carcinoma	U	+
018	Mixed undifferentiated and signet ring cell carcinoma, grade III, pT4aN3a	-	+
019	High-grade B-cell lymphoma	U	+
020	Adenocarcinoma	-	+
021	R/O malignant tumor	U	+

#"+": detected; "-": not detected; "U": uncertain of *H. pylori* infection. RC*: with "+" or without "-" inverse correlation between *DLL1* methylation and expression (data taken from Fig. 2).

Table 2. Relative qMSP primers used

Gene (RefSeq)	Primer Name	5'-Sequence	Detection	TM (°C)
GAPDH (NM_002046)	H_GAPDH_RT_F	CCCCTTCATTGACCTCAACTAGAT	RT-PCR Control	58, 54
	H_GAPDH_RT_R	CGCTCCTGGAAGATGGTGA		
Col2A1 (NM_0033150)	BR_137	TCTAACAATTATAAACTCCAACCACCAA	MSP Control	60
	BR_138	GGGAAGATGGGATAGAAGGGAATAT		
DLL1 (NM_005618.3)	DLL1_MSP_prom_F	GGTAGAGCGTAGGGGAATTC	MSP	60
	DLL1_MSP_prom_R	ACCCGATATCACTCGACGAC		
	DLL1_MSP_1stExon_F	AAGTCGGCGATTTTTATTTTTTC	MSP	60
	DLL1_MSP_1stExon_R	CAAAACTTCTTTCTTTAAAAACCGAT		
	DLL1_RT_F	TATCCGCTATCCAGGCTGTC	RT-PCR	58, 54
	DLL1_RT_R	GGTGGGCAGGTACAGGAGTA		

3-phosphate dehydrogenase (*GAPDH*) (NM_002046) reverse transcription primers (Table 2). A serial dilution of the *GADPH*-amplified cDNA was used to generate a standard curve, and *GAPDH* from each sample was used as a quantification control.

Generation of Myc-Tagged Notch1 Construct, Transfection, Clone Isolation and Cell Proliferation Assay

Myc-tagged Notch1 intracellular domain (Notch1

active domain, NCID) was cloned into a PiggyBac vector (9) and validated by sequencing. AGS cells were transfected with a control PiggyBac vector or the Myc-tagged NICD PiggyBac vector. The plasmid DNA was transfected by DMRIE-C (Invitrogen) transfection reagent in serum-free medium. The transiently transfected cells were then subjected to a cell proliferation assay or were selected with 2.4 μg/ml puromycin (Sigma-Aldrich) for stable clone isolation. Twelve individual control and twelve NICD-expressing clones were isolated and validated by their enhanced green fluorescent protein (EGFP) and expression of the Myc-tag. Serial dilutions of cells (10^{5-0}) were plated into each well of a 96-well assay plate and the cells were allowed to attach. Cells were then incubated at 37°C for 2 days. 3-(4,5-Dimethylthiazol-2-yl)-2,5-diphenyltetrazolium bromide (MTT) solution (20 μl, 5 mg/ml) (Sigma-Aldrich) was added to each well in 96-well plates and incubated at 37°C for 5 h. The reaction was terminated by adding 100 μl DMSO and light absorbance was measured at 595 nm.

Western Blot Analysis

Cells were harvested with the standard RIPA buffer (20 mM Tris, pH 7.5, 150 mM NaCl, 1 mM EDTA, 1% NP40, 0.5% DOC, 0.1% SDS), and denatured proteins were separated on a 10% polyacrylamide gel and trans-blotted onto a polyvinylidene difluoride (PVDF) membrane (Bio-Rad). After blocking with skim milk, the membrane was treated with antibodies directed against Notch1 (3608, which detects the mature Notch1 receptor) (Cell Signaling, MA, USA), myc-tag (05-724, which detects ectopically expressed NICD) (Millipore, CA, USA) and GAPDH (GeneTex, CA, USA). After washing, a secondary antibody conjugated with horseradish peroxidase was used to detect hybridization. Results were visualized by chemiluminescence. The film was scanned and analyzed.

Tissue Array and Immunostaining

Paraffin-embedded samples were prepared as described by Lu *et al.* (17). Tissue arrays were prepared by the Expensive Advanced Instrument Core Laboratory, Department of Medical Research and Development, Chang Gung Memorial Hospital at Chiayi, Taiwan. The sections were deparaffinized with xylene three times for 10 min each. The slides were then treated with 100% alcohol twice for 5 min each. After putting into a serial dilution of alcohol (95, 85, 70, 50, and 30%) for 3 min each, the slides were submerged in sterile water. The slides were then kept at 95-100°C in 10 mM citrate buffer (pH 6.0) for 10-20 min. The slides were then cooled to room temperature. After being submerged in phosphate buffered saline containing Tween-20 (PBST) twice for 3 min each time, the slides were placed in 3% hydrogen peroxide/methanol for 20 min. After being rinsed twice with PBST, the slides were blocked with of 10% goat serum/PBST. The slides were then treated with primary antibodies at 4°C overnight. After being washed with PBST three times for 2 min each time, 2 drops of biotinylated secondary antibodies were applied onto the slides. After 10 min, the slides were washed three times with PBST and one drop of 3,3'-Diaminobenzidine (DAB) substrate was applied. After washing and dehydration in the air, the slides were mounted. For fluorescence staining, the secondary antibodies used were conjugated with fluorescein and the mounting medium contained 4',6-diamidino-2-phenylindole (DAPI, Vector Laboratories, CA, USA). The photo-images were taken by conventional microscopy with both visible and different fluorescent light sources. Quantification of the image intensity was obtained from 10 fluorescent photos using the NIH Image software (https://imagej.nih.gov/nih-image). The obtained *DLL1* intensity was normalized with the obtained F-actin staining intensity from the fluorescence staining. Pathologists scored the expression intensity and expression area (percentage) of the tissue array. The intensity are listed 1, 2 or 3 in scale but the 1.5 and 2.5 scales were specifically pointed out by the pathologist. The expression area is rated from 10, 20, till 100% discretely.

Tumor Growth In Vivo

Isolated 10^6 control or NICD-expressing AGS cells were mixed with Matrigel (3:1) and inoculated subcutaneously into immune-deficient mice (BALB/cAnN.Cg-*Foxnl*^{nu}/CrlNarl, National Applied Research Laboratories, Taiwan). The mice were raised for 3 months. A fluorescence molecular tomography system (FMT) (PerkinElmer, CA, USA) was used to track and quantify an injected tumor tracking dye, IntegriSense 750 (PerkinElmer).

Statistics

A paired Student's *t*-test was used to compare the difference between the methylation and expression states.

Results

DLL1 Methylation in Gastric Cancer Cell Lines and Pre-Cancerous Samples

In order to detect the methylation state and expression pattern of *DLL1*, six gastric cancer cell lines, including AGS, KATOIII, MKN28, MKN45,

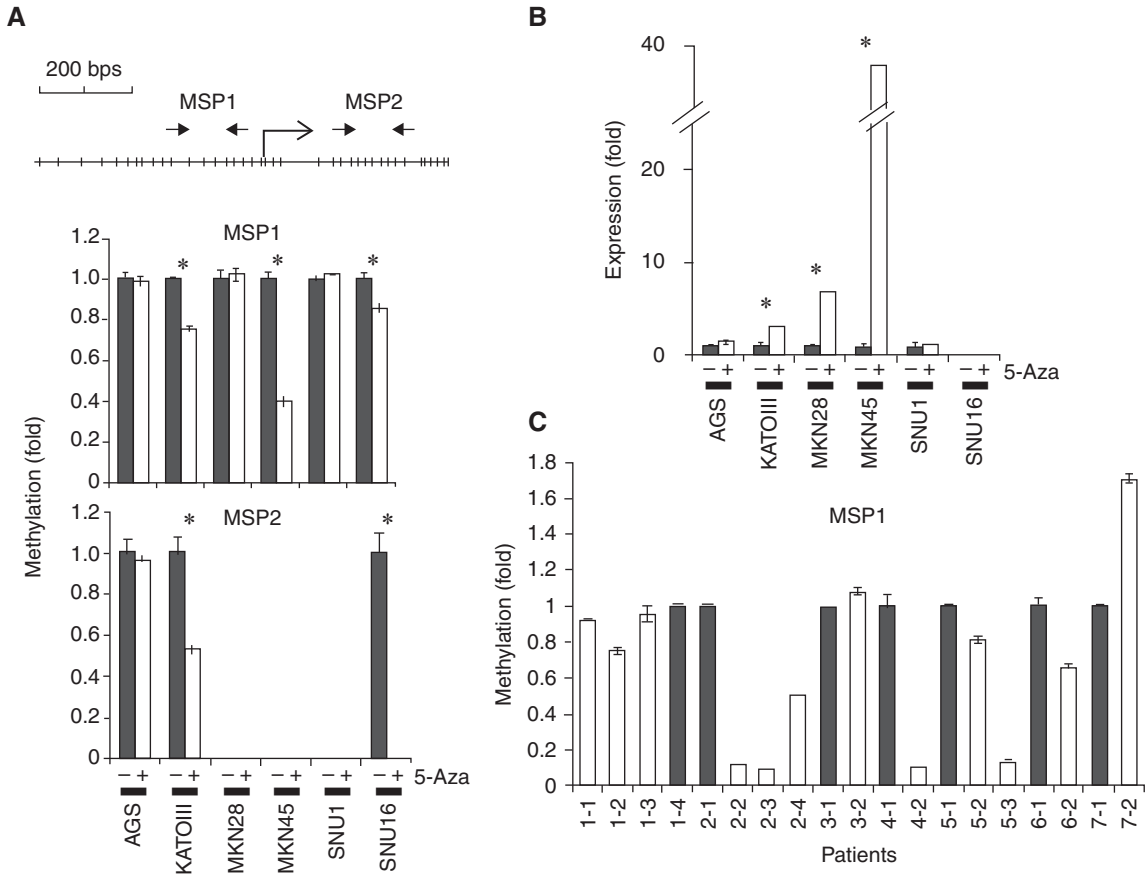

Fig. 1. *DLL1* methylation in gastric cancer cell lines and clinical samples. (A) Two pairs of relative qMSP primers were designed to detect the methylation states of the *DLL1* promoter and the first exon of the gene by relative-qMSP in the designated cancer cell lines before (-, filled columns) and after (+, open columns) 5-Aza treatment. In the upper panel, vertical bars indicate the CpG sites, the bended arrow indicates the transcriptional start site. (B) qRT-PCR was used to detect the *DLL1* expression before (-, filled columns) and after (+, open columns) 5-Aza treatment. (C) Relative-qMSP was used to detect *DLL1* methylation differences in seven gastric clinical samples (open columns) and one or more samples obtained from the normal regions (closed columns) of the same patient. The methylation percentages of the tumor samples were normalized by the methylation state of the normal regions for each patient to deduce the methylation fold changes. (n = 3, $*P < 0.05$)

SNU1 and SNU16, were treated with 5 μM 5-Aza for 5 days. Two MSP primers were designed to determine and quantify the methylation state of the *DLL1* promoter (MSP1, Fig. 1A) and first exon region (MSP2, Fig. 1A). MSP1 detected significant demethylation in the promoter region in the KATOIII and MKN45 cell lines (Fig. 1A center), also in the exon 1 region in MKN28, MKN45 and SNU1 cell lines (Fig. 1A, bottom panel). *DLL1* expression was significantly increased after demethylation in the KATOIII, MKN28, and MKN45 cell lines (Fig. 1B), reflecting demethylation of these cells lines shown in Fig. 1A. Therefore, *DLL1* methylation was identified in several of the gastric cancer cell lines.

The MSP1 primers were next used to detect the *DLL1* methylation state in pre-cancerous samples. The results found that there were significant *DLL1* hypermethylation in the pre-malignant (Fig. 1C, open columns) compared with the adjacent normal (Fig. 1C. filled columns) regions. In order to determine correlation between *DLL1* expression and methylation in the pre-cancerous clinical samples, relative-qMSP and immunostaining were performed (Fig. 2 and Table 1). After quantification, a reverse correlation was found between the methylation state and *DLL1* expression.

Abnormal DLL1 Expression in Gastric Cancer Samples

To confirm that *DLL1* was abnormally expressed in gastric cancers, 40 pairs (tumor versus adjacent normal) of gastric cancer clinical samples were collected and arrayed. After immunostaining (Fig. 3A) and analysis, *DLL1* expression intensity was given

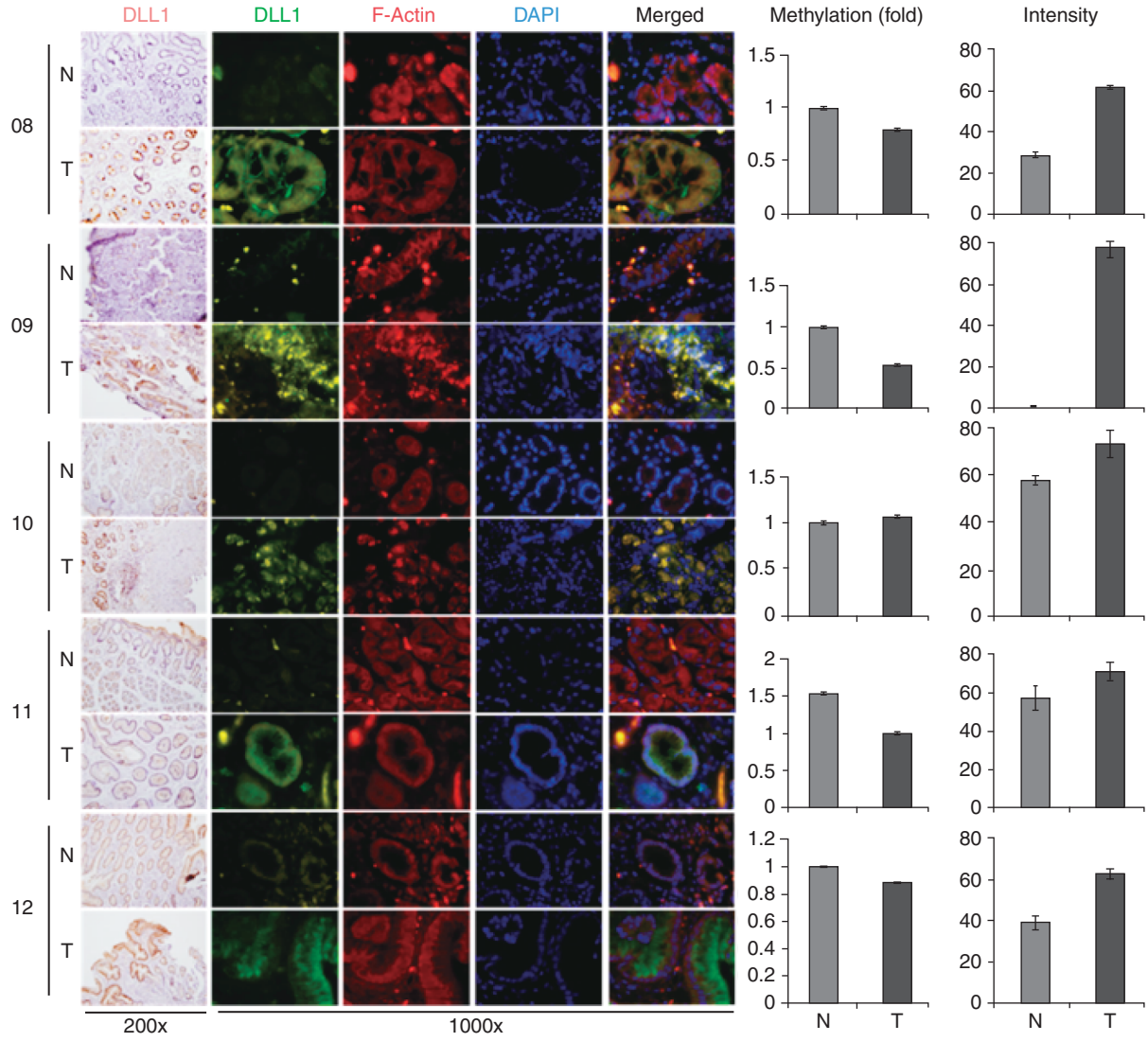

Fig. 2. Reverse correlation between *DLL1* methylation and expression levels. Paraffin sections were prepared from patient premalignant samples (patient numbers 8-12) and immunostained by DAB subtract (left column) or designated conjugated fluorescents. Intensity of the fluorescents was obtained from the digital photos and analyzed by NIH Image (Image J). Relative qMSP was used to detect the respective methylation states from the collected samples. The black and white scale bars represent the length of 60 and 10 μm, respectively. N and T denote normal and tumor samples. The intensity was measured with NIH Image.

a score of 1-3 and the expression area was scored by percentage. In a paired *t*-test, the expression intensity of *DLL1* was significantly decreased in the tumor (Fig. 3B), while the expression area showed no significant differences between the normal and tumor regions (Fig. 3C). In individual samples, *DLL1* was found to be more highly expressed in the normal than in the tumor regions in the majority of the clinical samples of all four stages (Fig. 3D). Furthermore, *DLL1* expression was significantly less in the *H. pylori*-positive than in the *H. pylori*-negative samples (Fig. 3E).

NICD Overexpression Suppressed Tumor Cell Proliferation in vitro but Enhanced Tumor Growth In Vivo

In order to evaluate the pathological functions of Notch signaling, NICD, which is the active form of Notch1 downstream of the *DLL1* signal, was cloned into a PiggyBac vector (Fig. 4A, left panel) and sequence-validated. Control (PiggyBac only) and NICD-expressing PiggyBac constructs were transfected into AGS gastric cancer cells. Twelve control and twelve NICD-expressing AGS clones were isolated based on puromycin resistance and

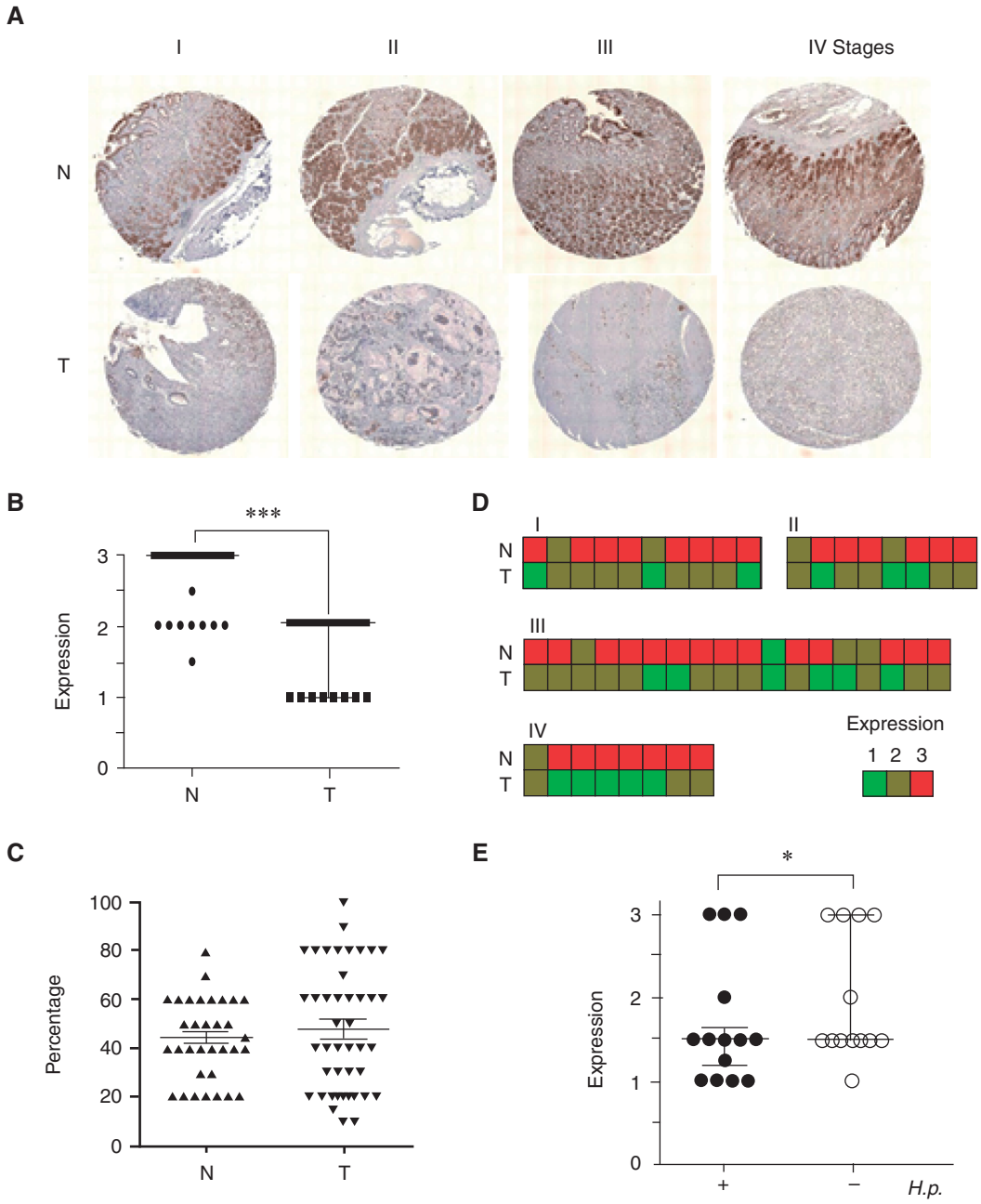

Fig. 3. Abnormal *DLL1* expression detected by tissue array. (A) Forty pairs of gastric cancer samples were arrayed and immunostained with anti-*DLL1* antibodies. The stained slides were scanned and examined by a pathologist. *DLL1* expression intensity was scored 0-3, while expression area was scored by percentage from each block of samples. (B) Relative *DLL1* expression intensity from paired normal and tumor regions was compared (paired t-test). (C) *DLL1* expression percentage from paired normal and tumor regions was compared. (D) *DLL1* expression intensity from individuals collected from four stages of gastric cancer (I-IV) is shown as a heatmap. (E) Comparison of the *DLL1* expression intensity between *H. pylori* (*H.p*)-detected (+) or non-detected (-) gastric samples.

EGFP expression. Myc-tagged NICD expression was validated by western blot analysis (Fig. 4A, right panel). Control- and NICD-transiently transfected AGS cells were tested for their proliferation capacity by the MTT assay. The results showed that proliferation of the AGS cells was suppressed after NICD transient transfection (Fig. 4B). The same proliferation suppression was observed in the isolated NICD-expressing clones (represented by Notch1 _1, _3 and _12 in Fig. 4C).

The stable control and NICD-expressing AGS clones (10^6 cells) were then inoculated subcutane-

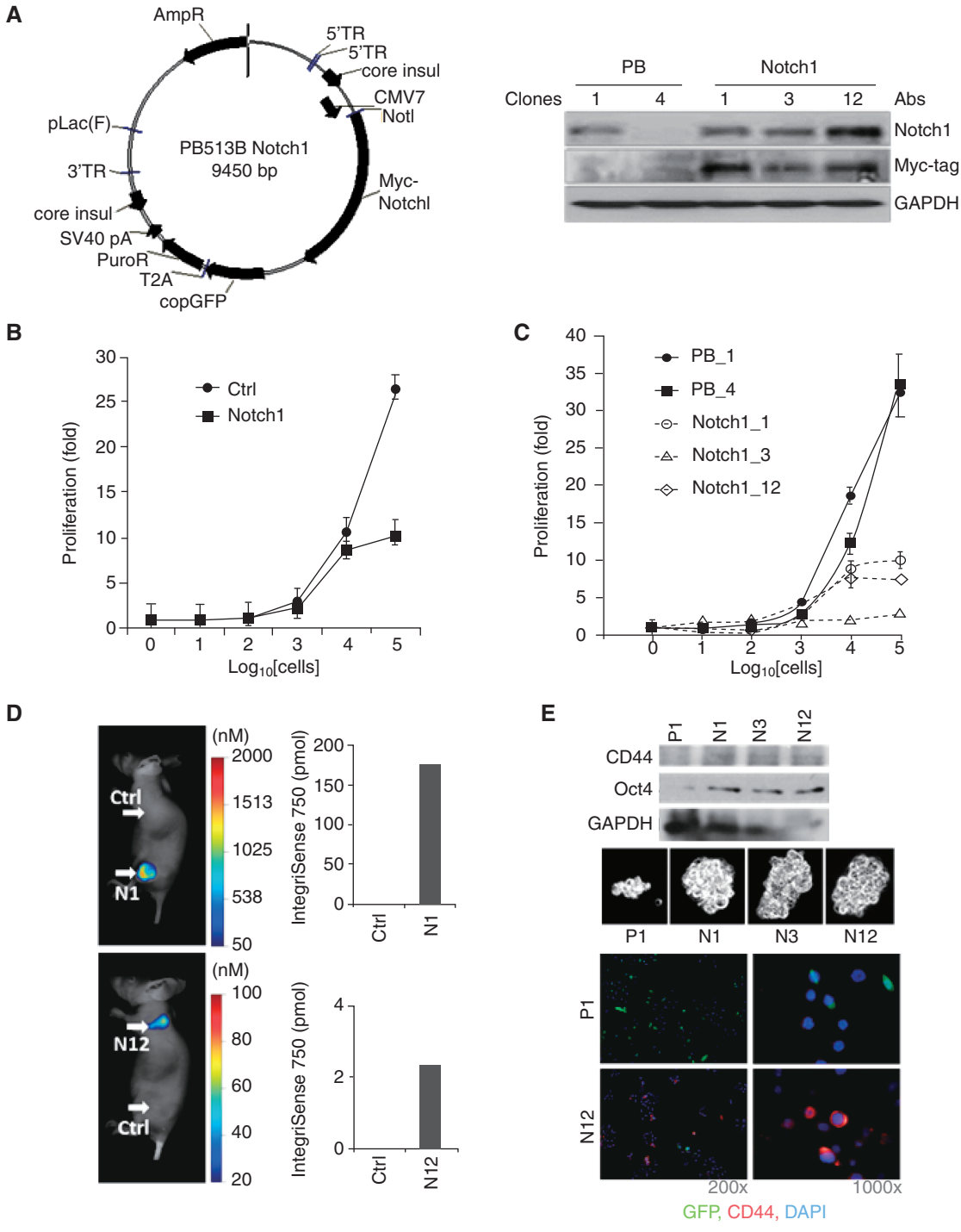

Fig. 4. NICD overexpression in the AGS gastric cancer cell line. (A) Left panel, Physical map of Myc-tagged NICD in the PiggyBac vector. Right panel, western blot validation of the Notch overexpression in randomly isolated clones. Proteins from isolated control (PiggyBac vector only, PB) and Notch1-overexpressed (Notch1) clones were subjected to western blot analysis. Antibodies against Notch1, Myc-taq or GAPDH was used to probe the expression of the target genes. (B) Proliferation of the control (circle)- or NICD (square) transiently-transfected AGS cells. (C) Proliferation of the isolated control (closed) or NICD-overexpressing (open) clones of AGS cells. Two controls and three NICD clones were analyzed. (D) NICD overexpression affected tumor growth *in vivo*. Control and NICD-overexpressing AGS cells (10^6 cells each) were mixed with Matrigel and injected subcutaneously into immune-deficient mice. After 3 months of tumor growth, the mass of the tumor of the mice (left panels) was quantified (right panels) by the intensity of an injected cancer tracking dye (IntegriSense 750) in a FMT system. (E) Expression of Oct4 and CD44 tumor stem cell-like markers in Notch-overexpressed AGS cells. Western (upper panel) and immunostaining (lower panel) were used to detect the enhanced Oct4 and CD44 expression in Notch-overexpressed AGS cells. The enhanced Oct4 and CD44 expression correlates with the enhanced sphere-formation in low attachment dishes (center panel). In (C) and (E), N1, N3 and N12 were Notch1-1, -3 and -12, respectively, and P1 was PB-1 of (C) above. These were all isolated Notch-expressing or vector-insertion AGS stable clones.

ously into immune-deficient mice and tumor growth was monitored for 3 months (n = 4). We found that the tumor growth was enhanced in the NICD-expressing clones, while the control clones did not develop into tumors (Fig. 4D). These data indicate that sustained Notch signaling enhances tumor growth *in vivo*.

Notch signaling is responsible for stem cell maintenance and there are reports that Notch signaling is associated with a tumor stem cell-like phenotype (2, 11, 21). The proliferation of NICD-overexpressing AGS cells was suppressed, but these cells formed tumors in the xenograft model. While this seems contradictory, the data did correlate with the slow-growing but tumorigenic capacity of cancer stem cell-like cells (2, 11, 21). In this study, we observed upregulated expression of the stem cell markers Oct4 and CD44 in NICD-overexpressing AGS clones (N1, 3 and 12 in Fig. 4E compared with PB1), which indicates that NICD overexpression might result in the gastric cancer cells being more cancer stem cell-like.

Discussion

In the current study, abnormal *DLL1* methylation and a reverse correlation with *DLL1* expression was identified in gastric cancer cell lines and tumor samples. The collected gastric cancer clinical samples might be infected with microorganisms to lower the RNA integrity. Hence, immunohistochemical staining, instead of qRT-PCR, was used to detect *DLL1* expression in clinical tissues. Abnormal *DLL1* methylation has been described in different cancers including gastric cancer (13, 18), while most of the previous studies have focused on abnormal *DLL4* expression (20). In this study, 5-Aza treatment caused various degrees of demethylation in the *DLL1* promoter (MSP1) and first exon (MSP2) (Fig. 1), suggesting differential methylation states in the different gastric cancer cell lines analyzed. Since DNA methylation is an inheritable dominant silencing mark, the finding of abnormal *DLL1* methylation states in gastric cancer suggests that epigenetic regulation of Notch signaling might be involved in gastric tumorigenesis.

Compared with the consistent decrease in *DLL1* expression in gastric cancer samples, the abnormal methylation and expression of *DLL1* was not consistently observed in gastric pre-cancerous lesions. This observation suggests that Notch signaling might play different roles in individual cases of gastric lesions and during the very early stages of transformation. In other solid tumors, such as breast, colorectal, pancreatic, cervical, oral squamous cell carcinoma (SCC) and lung cancer, Notch signaling is suggested to be involved in the oncogenic process (21). However, Notch acts as a tumor suppressor in prostate, liver, glioblastoma and skin cancer (16). Hence, contradictory data indicate that Notch signaling could be both oncogenic and tumor suppressing in breast and lung cancers. Therefore, it is important to monitor abnormal *DLL1* methylation/expression and possible pathological development in different patients with gastric lesions.

Reports have indicated that that Notch signaling is associated with stem cell maintenance and tumor stem cell-like phenotype (2, 11, 21). Suppressed proliferation and tumor formation in the xenograft model and analysis of expression of the stem cell marker genes, Oct 4 and CD44, suggested the NICD-expressed AGS cells could have become cancer stem cell-like. More cells expressing Oct4 and CD44 in NICD-overexpressing AGS clones (Fig. 4E) indicate that NICD overexpression might transform the gastric cancer cells to become more cancer stem cell-like.

In conclusion, an inverse correlation between abnormal *DLL1* methylation and expression was observed in gastric pre-cancerous lesions. *DLL1* expression was lower in the tumor regions than in the paired normal regions in clinical samples from all four stages of gastric tumors. NCID overexpression suppressed cell proliferation in cultured cells but promoted tumor growth in immune-deficient mice.

Conflicts of Interest

The authors declare no conflicts of interest.

Acknowledgments

All the works were supported by Chang Gung Memorial Hospital (CORPG6D0051, CORPG6D0052, and CORPG6D0053).

References

1. Ables, J.L., Breunig, J.J., Eisch, A.J. and Rakic, P. Not(ch) just development: Notch signalling in the adult brain. *Nat. Rev. Neurosci*. 12: 269-283, 2011.
2. Ayyanan, A., Civenni, G., Ciarloni, L., Morel, C., Mueller, N., Lefort, K., Mandinova, A., Raffoul, W., Fiche, M., Dotto, G.P. and Brisken, C. Increased Wnt signaling triggers oncogenic conversion of human breast epithelial cells by a Notch-dependent mechanism. *Proc. Natl. Acad. Sci. USA* 103: 3799-3804, 2006.
3. Baylin, S.B. and Ohm, J.E. Epigenetic gene silencing in cancer - a mechanism for early oncogenic pathway addiction? *Nat. Rev. Cancer* 6: 107-116, 2006.
4. Bibikova, M., Chudin, E., Wu, B., Zhou, L., Garcia, E.W., Liu, Y., Shin, S., Plaia, T.W., Auerbach, J.M., Arking, D.E., Gonzalez, R., Crook, J., Davison, B., Schulz, T.C., Robins, A., Khanna, A., Sartipy, P., Hyllner, J., Vanguri, P., Savant-Bhonsale, S., Smith, A.K., Chakravarti, A., Maitra, A., Rao, M., Barker, D.L., Loring, J.F. and Fan, J.B. Human embryonic stem cells have a unique epigenetic signature. *Genome Res*. 16: 1075-1083, 2006.
5. Chenn, A. and McConnell, S.K. Cleavage orientation and the asymmetric inheritance of Notch1 immunoreactivity in mammalian neurogenesis. *Cell* 82: 631-641, 1995.
6. Date, S. and Sato, T. Mini-gut organoids: reconstitution of the stem cell niche. *Annu. Rev. Cell Dev. Biol*. 31: 269-289, 2015.

7. Ehrlich, M. Cancer-linked DNA hypomethylation and its relationship to hypermethylation. *Curr. Top. Microbiol. Immunol*. 310: 251-274, 2006.
8. Hsiao, S.H., Huang, T.H. and Leu, Y.W. Excavating relics of DNA methylation changes during the development of neoplasia. *Semin. Cancer Biol*. 19: 198-208, 2009.
9. Hsu, K.W., Hsieh, R.H., Huang, K.H., Fen-Yau Li, A., Chi, C.W., Wang, T.Y., Tseng, M.J., Wu, K.J. and Yeh, T.S. Activation of the Notch1/STAT3/Twist signaling axis promotes gastric cancer progression. *Carcinogenesis* 33: 1459-1467, 2012.
10. Kang, C., Song, J.J., Lee, J. and Kim, M.Y. Epigenetics: an emerging player in gastric cancer. *World J. Gastroenterol*. 20: 6433-6447, 2014.
11. Katoh, M. Dysregulation of stem cell signaling network due to germline mutation, SNP, Helicobacter pylori infection, epigenetic change and genetic alteration in gastric cancer. *Cancer Biol. Ther*. 6: 832-839, 2007.
12. Katoh, M. Notch signaling in gastrointestinal tract (review). *Int. J. Oncol*. 30: 247-251, 2007
13. Ku, J.L. and Park, J.G. Biology of SNU cell lines. Cancer Res. *Treat*. 37: 1-19, 2005.
14. Leu, Y.W., Yan, P.S., Fan, M., Jin, V.X., Liu, J.C., Curran, E.M., Welshons, W.V., Wei, S.H., Davuluri, R.V., Plass, C., Nephew, K.P. and Huang, T.H. Loss of estrogen receptor signaling triggers epigenetic silencing of downstream targets in breast cancer. *Cancer Res*. 64: 8184-8192, 2004.
15. Li, H., Mo, J., Jia, G., Liu, C., Luan, Z. and Guan, Y. Activation of Wnt signaling inhibits the pro-apoptotic role of Notch in gastric cancer cells. *Mol. Med. Rep*. 7: 1751-1756, 2013.
16. Lobry, C., Oh, P., Mansour, M.R., Look, A.T. and Aifantis, I. Notch signaling: switching an oncogene to a tumor suppressor. *Blood* 123: 2451-2459, 2014.
17. Lu, C.K., Lai, Y.C., Chen, H.R. and Chiang, M.K. Rbms3, an RNA-binding protein, mediates the expression of Ptf1a by binding to its 3'UTR during mouse pancreas development. *DNA Cell Biol*. 31: 1245-1251, 2012.
18. Piazzi, G., Fini, L., Selgrad, M., Garcia, M., Daoud, Y., Wex, T., Malfertheiner, P., Gasbarrini, A., Romano, M., Meyer, R.L., Genta, R.M., Fox, J.G., Boland, C.R., Bazzoli, F. and Ricciardiello, L. Epigenetic regulation of Delta-Like1 controls Notch1 activation in gastric cancer. *Oncotarget* 2: 1291-1301, 2011.
19. Previs, R.A., Coleman, R.L., Harris, A.L. and Sood, A.K. Molecular pathways: translational and therapeutic implications of the Notch signaling pathway in cancer. *Clin. Cancer Res*. 21: 955-961, 2015.
20. Qian, C., Liu, F., Ye, B., Zhang, X., Liang, Y. and Yao, J. Notch4 promotes gastric cancer growth through activation of Wnt1/beta-catenin signaling. *Mol. Cell. Biochem*. 401: 165-174, 2015.
21. Ranganathan, P., Weaver, K.L. and Capobianco, A.J. Notch signalling in solid tumours: a little bit of everything but not all the time. *Nat. Rev. Cancer* 11: 338-351, 2011.
22. Saga, Y. and Takeda, H. The making of the somite: molecular events in vertebrate segmentation. *Nat. Rev. Genet*. 2: 835-845, 2001.
23. Satolli, M.A., Buffoni, L., Spadi, R. and Roato, I. Gastric cancer: The times they are a-changin'. *World J. Gastrointest. Oncol*. 7: 303-316, 2015.
24. Toyoda, T., Tsukamoto, T., Yamamoto, M., Ban, H., Saito, N., Takasu, S., Shi, L., Saito, A., Ito, S., Yamamura, Y., Nishikawa, A., Ogawa, K., Tanaka, T. and Tatematsu, M. Gene expression analysis of a Helicobacter pylori-infected and high-salt diet-treated mouse gastric tumor model: identification of CD177 as a novel prognostic factor in patients with gastric cancer. *BMC Gastroenterol*. 13: 122, 2013.
25. Valk-Lingbeek, M.E., Bruggeman, S.W. and van Lohuizen, M. Stem cells and cancer; the polycomb connection. *Cell* 118: 409-418, 2004.
26. Yan, P.S., Venkataramu, C., Ibrahim, A., Liu, J.C., Shen, R.Z., Diaz, N.M., Centeno, B., Weber, F., Leu, Y.W., Shapiro, C.L., Eng, C., Yeatman, T.J. and Huang, T.H. Mapping geographic zones of cancer risk with epigenetic biomarkers in normal breast tissue. *Clin. Cancer Res*. 12: 6626-6636, 2006.